Aperture-Based Daylight Modelling
Evaluating the Airmass Refinement for the Sunlight Beam Index

Mardaljevic, J.; Brembilla, E.

DOI
10.26868/25222708.2021.30604

Publication date
2022

Document Version
Final published version

Published in
BS 2021 - Proceedings of Building Simulation 2021

Citation (APA)
Mardaljevic, J., & Brembilla, E. (2022). Aperture-Based Daylight Modelling: Evaluating the Airmass Refinement for the Sunlight Beam Index. In D. Saelens, J. Laverge, W. Boydens, & L. Helsen (Eds.), *BS 2021 - Proceedings of Building Simulation 2021: 17th Conference of IBPSA* (pp. 342-349). (Building Simulation Conference Proceedings). International Building Performance Simulation Association. https://doi.org/10.26868/25222708.2021.30604

Aperture-Based Daylight Modelling: Evaluating the Airmass Refinement for the Sunlight Beam Index

J Mardaljevic[1], E Brembilla[2]
[1]Loughborough University, Loughborough, UK
[2]Delft University of Technology, Delft, The Netherlands

Abstract

Aperture-based daylight modelling (ABDM) is a new building simulation paradigm founded on measures of an aperture's 'connectedness' to the sun and the external environment. At the planning level, there currently does not exist anywhere an evaluative schema which is equally applicable to measures of solar energy potential (for PV performance, overheating risk, etc) and measures of sunlight/daylight amenity (for daylight, well-being, connectivity/view, etc). ABDM addresses that shortcoming. This paper describes the latest development of ABDM which is the addition of an airmass factor in the computation of the sunlight beam index (SBI). This enhancement preserves the 'geometrical purity' of ABDM, but now airmass SBI can serve as a reliable proxy for direct sun irradiation totals derived from weather files.

Key Innovations

- An airmass factor is introduced into the formulation of the (purely geometrical) sunlight beam index (SBI).
- A way of relating direct solar irradiation totals to airmass SBI is described and tested.
- Airmass SBI is shown to serve as a reliable proxy for (location specific) direct solar irradiation with the application of a single factor derived from weather files.
- A time-step dependancy on the determination of east–west totals of direct solar irradiation from weather files was (serendipitously) discovered.

Practical Implications

The airmass refinement for the sunlight beam index allows this, essentially geometrical, metric to serve both as a basis for sunlight planning decisions and also an indicator of performance measures such as PV generation potential.

Introduction

The European standard EN 17037 for daylight in buildings was approved by country vote in 2018. By June 2019 it was given the status of a national standard for all participating countries – with the proviso, if deemed necessary, of a national annex. The Introduction to the standard begins with the assertion that: *"Daylight should be a significant source of illumination for all spaces with daylight opening(s)."* (British Standards Institute (2018)) It continues: *"Daylight openings provide views and connection to the outside and contribute to the psychological well-being of occupants. A daylight opening can also provide exposure to sunlight indoors, which is important, for example, in dwellings, hospital wards and nurseries."* The word "opening" appears 139 times in the standard. This paper describes the latest development in a fundamental reconsideration of the way in which a building opening (or any surface) can be evaluated in terms of its potential to provide: sunlight, skylight and views. The means of evaluation in each case are essentially geometrical. The approach, designated Aperture-Based Daylight Modelling (ABDM) in 2019, was conceived to provide a significant upgrade over any of the methodologies traditionally used in planning guidelines for daylight/-sunlight. Though radical in conception, the theoretical basis of new approach is actually remarkably simple. So simple in fact that, to many, it may seem long-overdue.

Outline of the skylight and view indices

This paper focuses on the enhancement to the sunlight beam index, however a brief overview of the skylight and view indices is given here to set the sunlight beam index within the wider context of the aperture-based daylight modelling approach. Readers are directed to other papers for fuller descriptions of what is given below: Mardaljevic (2019, 2020).

The aperture skylight index (ASI) was conceived as a measure of the 'connectedness' of an aperture to the sky vault in terms of illumination received from a uniform luminance sky (Mardaljevic (2017)). Recognition that direct view of the sky is the primary determinant of daylight illumination was made in the sixth of Vitruvius' (c. 90–c. 20 BC) Ten Books on Architecture. Vitruvius gives a recommendation to determine a measure related to what would now be called the 'no

https://doi.org/10.26868/25222708.2021.30604

sky line' – a still commonly used rule of thumb. The ASI can be thought of as akin to an integral measure of the no-sky line taken at the aperture. The illuminance across the aperture was chosen in preference to, say, the solid angle of sky visible at the aperture for a number of reasons:

1. Illuminance received at the aperture relates more directly to the illumination potential of the aperture than solid angle because it already includes the cosine weighting of the visible sky.
2. The determination of solid angle has to be made at a point, say, the middle of the aperture, whereas the illuminance can be determined across the entire aperture.
3. The use of illuminance determined across the aperture allows for accurate evaluation of arbitrarily complex shading structures, e.g. brise-soleil.

The CIE standard overcast sky formulation was not used because it is in fact an "extreme" type of overcast sky that occurs in reality much less often than its commonplace usage for daylight evaluations might suggest (Enarun and Littlefair (1995)). To account for the size of the aperture, its 'connectedness' with the sky vault is calculated in terms of the lumens received across the aperture. The uniform sky used was normalised to 2000 lux on the the horizontal. This arbitrary normalisation was chosen so that each square metre of vertical aperture can receive a maximum of 1000 lumens from the sky. Application is illustrated in Figure 1 where the lumens received for a 1m^2 vertical aperture in three settings is shown. The false-colour map shows the distribution of illuminance across the aperture for: (a) a thin wall (i.e. unobstructed); (b) a 20 cm reveal; and, (c) with the further addition of a 50 cm overhang. The annotation gives the lumens received by the aperture: 1000, 690 and 530 lm for each respective setting. Evident is the reduction in lumens received – and therefore reduced potential for (direct) diffuse skylight – produced by the obstructions.

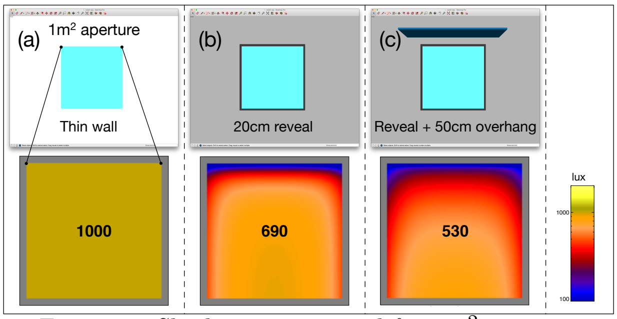

Figure 1: Sky lumens received for 1m^2 aperture

In Mardaljevic (2019) the concept of the 'view lumen' was introduced. This proposed that the measure of an aperture's 'connectedness' to the sky (i.e. the lumens received) is in fact a proxy measure of the potential view (to the sky) from that aperture. Thus, it is a straightforward matter to extend the ASI approach to determine an aperture's 'connectedness' to all three key layers that provide the components of view: ground, foreground (e.g. buildings) and sky. To achieve this, the geometry that comprises each of the view layers is made luminous, and the flux of illumination from each layer (received at the aperture and averaged across it) serves as proxy measures of view (from the aperture) for each of the view layers, Figure 2.

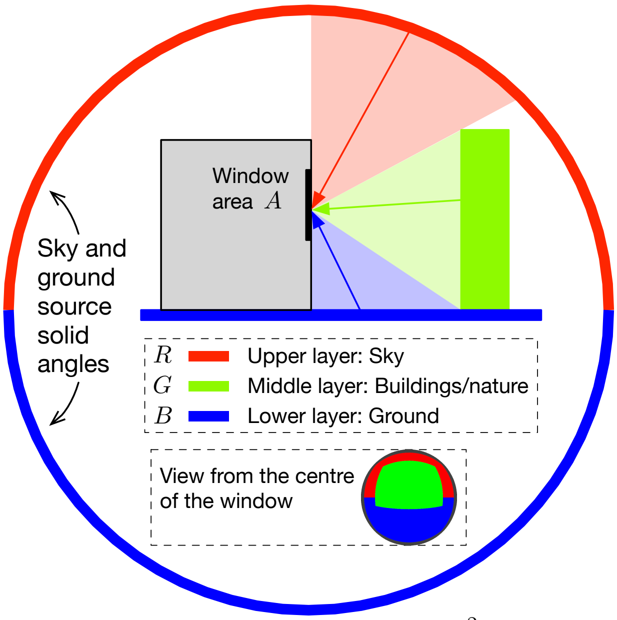

Figure 2: Sky lumens received for 1m^2 aperture

The sunlight beam index

The sunlight beam index (SBI) was originally conceived as a means to rate a window aperture's potential to receive sunlight for planning and solar access purposes, Mardaljevic and Roy (2016). The sunlight beam index is a measure of an aperture's 'connectedness' to all of the annually occurring possible sun positions where sunlight can be incident on the aperture (Mardaljevic and Roy (2016)). A single, unambiguous measure of sunlight beam potential forms the basis of the sunlight beam index (SBI). The annual SBI is the cumulative measure of the cross-sectional area of sunbeam that can pass through a window aperture over the period of a full year. It accounts for all the possible above horizon sun positions and is determined on an hourly or sub-hourly basis. SBI therefore has a temporal dimension and can be decomposed into a series of shorter aggregate time periods, e.g. 12 monthly totals, 24 monthly am and pm totals, etc.

With the area given in square metres and the time period given in hours (or more typically, a fraction of an hour), the sunlight beam index (SBI) has units of m^2 hrs. This formulation makes good sense for a number reasons:

https://doi.org/10.26868/25222708.2021.30604

- It is consistent with fundamental illumination physics (e.g. the cosine law of illuminance as a proxy for reduced area of cross-sectional beam).
- The penetration depth of the sun's rays into the space will be reduced with increasing angle of incidence.
- Large incidence angle sun illumination on the window will have a proportionate (i.e. small) contribution in any evaluation without requiring any recourse for arbitrary cut-off conditions, e.g. 'dead angles', etc.
- The glazed area is properly accounted for.
- Shading – whatever its origin – is properly accounted for.

Any meaningful evaluation must account for the entire year of possible sun positions to capture all of the potential occurrences of sun and and, importantly, shading also. If required, the total SBI for a dwelling or building can be obtained by summing all SBIs for the relevant windows or window groups. Thus it becomes possible to characterise the sunlight beam index for an entire building (e.g. dwelling) with a *single* SBI value, Mardaljevic and Roy (2017).

In the original formulation of the sunlight beam index the highest instantaneous SBI occurs when the sun is normal to the aperture. For, say, a west-facing window, the highest SBI occurs around dusk when the sun is just above the horizon. The overriding design philosophy behind ABDM is simplicity; characterised by a basis that is purely geometrical, i.e. the 'connectedness' of an aperture to the three view layers and all of the possibly occurring sun positions. Notwithstanding the appeal of this formulation, the sunlight beam index possess an intrinsic drawback: for vertical apertures, low angle sun contributes strongly to the point in time and annual total SBI. Whilst it may be useful for the designer to know that the setting sun will be visible from a particular window, say, during the winter months, the temporal map conveys the impression that the greatest sun contribution will be when the sun is just above the horizon, i.e. at or near normal to the aperture. Similarly, any shading losses in terms of reduced annual total SBI will be greatest for obstruction of horizon sun.

Method: Airmass corrected SBI

The solution most in keeping with the ABDM ethos was to include an attenuation factor for SBI based on the airmass. The airmass (strictly, the airmass coefficient) describes the optical thickness of the atmosphere relative to that for the shortest path length (from sea level) directly upwards towards the zenith, Figure 3. For a horizontal view direction (e.g. to the sun at the horizon) the airmass is approximately 40× that toward the zenith. Factoring in the airmass gives a new measure of sunlight beam index referred to here as SBI-Airmass to distinguish it from the original formulation now designated SBI-Classic. It is hypothesised that SBI-Airmass can be related directly to cumulative measures of direct sun irradiation derived from weather files – this is tested in the sections that follow.

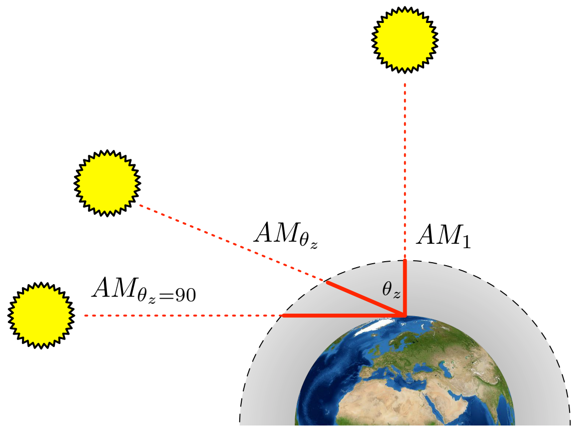

Figure 3: Airmass (AM) as a function of solar zenith angle θ_z

Of the many formulations for airmass currently available, it was decided in the first instance to employ the model presented by Kasten (1965). This is perhaps the most established of the empirically-based models that requires only a solar angle as input:

$$AM = \left[\cos\theta_z + 0.15\,(93.885 - \theta_z)^{-1.253}\right]^{-1} \quad (1)$$

where c is the solar zenith angle. (Kasten (1965)) Clear sky direct beam solar radiation I_{am} is determined from the airmass zero value I_0 using an empirical relationship which accounts for site elevation:

$$I_{am} = I_0\left[(1 - 0.14h)\,0.7^{AM^{0.678}} + 0.14h\right] \quad (2)$$

where h is the elevation above sea level in km. (Meinel and Meinel (1976); Laue (1970)) The relation is believed to be reliable for elevations up to 2 km and perhaps beyond. The SBI airmass factor f_{am} is then normalised to maximum terrestrial (i.e. unit airmass) beam irradiation I_1 determined at sea level (i.e. where $h = 0$ in equation 2):

$$f_{am} = \frac{I_{am}}{I_1} \quad (3)$$

Note, there are differences between the various models for predicting I_{am} as a function of solar angle. However, those resulting largely from differences between the direct beam maxima at the greatest solar altitude will be lessened in the schema described here because of the applied normalisation to the SBI airmass factor (equation 3).

Airmass for any particular solar angle can be considered an essentially intrinsic property for any given

https://doi.org/10.26868/25222708.2021.30604

site. In contrast, atmospheric turbidity is constantly changing due to varying levels of water vapour, dust, etc. In addition to the random variations in turbidity, there is also a strongly regional character at the global scale to prevailing levels and patterns of atmospheric turbidity. Notwithstanding the ready availability of monthly global maps for, say, the Linke turbidity coefficient[1] the dynamic nature of turbidity excludes it from consideration as an additional factor to attenuate direct sun in the SBI schema.

The SBI airmass factor f_{am} curves for three site elevations are shown in Figure 4. The airmass factor is plotted against solar altitude $\alpha_s = 90 - \theta_z$. For a site at sea level, the (instantaneous) SBI for the sun at the horizon is approximately 1/42 that of the sun at the zenith. For elevations above sea level the airmass

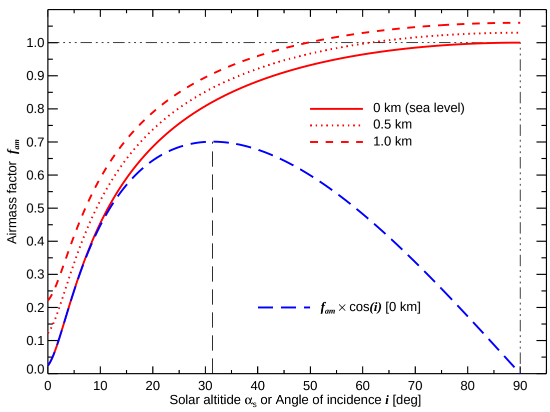

Figure 4: SBI airmass factor

factor achieves values greater than one. Also plotted is a curve of $f_{am} \times \cos(i)$ where i is the angle of incidence between the surface normal of the aperture and the sunlight beam (for 0 km elevation). For, say, a west facing vertical aperture, this curve shows the competing effect between increasing cross-section of sunlight beam (as the sun sets) and the reduction in intensity of the beam due to increasing airmass. Similarly, considering only sun positions at solar noon for a south facing aperture, the solar altitude is equal to the angle of incidence. With the airmass formulation used here (equation 2), the maximum SBI-AM will occur when the solar altitude equals 31.4° (vertical dashed line in Figure 4).

Results

The effect of including the airmass factor in the computation of SBI is illustrated in Figure 5 comparing temporal maps of SBI-Classic with SBI-Airmass for a 1 m^2 south facing aperture in London (UK). There are now two peaks in SBI around midday in March and October rather than a single peak in December – a consequence of the (blue) curve for airmass factor multiplied by the cosine of the angle of incidence (Figure 4). And, of course, the magnitude of the peaks in SBI-AM is lower than the peak in SBI-CL. The annual total SBI reduces from 1928 m^2 hrs (SBI-CL) to 1392 m^2 hrs (SBI-AM).

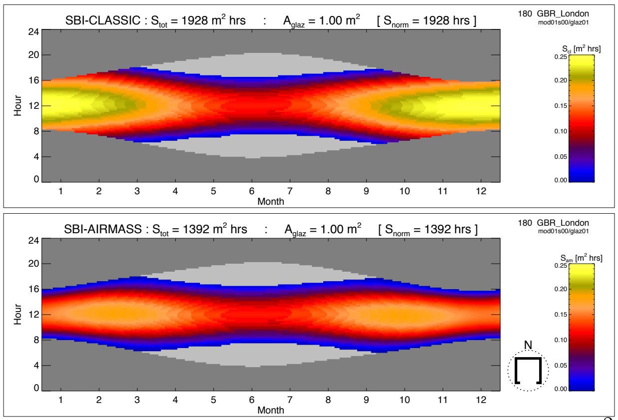

Figure 5: SBI airmass factor comparison for 1m^2 south facing, unobstructed aperture, London, UK)

SBI-Airmass and direct normal irradiation from weather files

A simple set of geometrical scenarios were devised to create variation in direct sun exposure to test the relation between annual totals for SBI-airmass and cumulative direct sun irradiation derived from weather files. Changes in direct sun exposure resulted from variation in two factors: scene orientation and the degree of partial occlusion caused by a (variable height) obstruction. The simple scene comprised a 1 m^2 aperture facing a 20 m wide obstruction placed 10 m away from it. The obstruction height was adjusted to give an elevation angle (from the middle of the aperture) of 0° (i.e. no obstruction); 20°; 40° and 60°, Figure 6(a)–(d). The sun exposure for each scene was determined for seven possible scene orientations: 45° to 315° in steps of 45°, Figure 6(e). Thus there were 28 combinations of scene obstruction and scene orientations. Note, the scenarios were designed to be symmetrical about the north-south axis.

A number of weather files selected more or less at random from the Climate.OneBuilding.Org website were evaluated as follows, each for all 28 combinations of scene obstruction and scene orientation. Total annual SBI-AM (T_{sam}) and weather file total annual direct sun irradiation (T_{wds}) on the 1 m^2 aperture was predicted using a bespoke *Radiance*-based CBDM/ABDM system known as the 4 Component Method. Though, for this evaluation the results are concerned only with the direct sun component. In the first instance, a time-step of 15 minutes was used for the simulation of both T_{sam} and T_{wds}. The direct normal irradiance time-series in the hourly weather files were rebinned to a 15 min time-step using linear interpolation.

For both the CBDM and ABDM parts (i.e. total annual direct sun irradiation and total annual SBI-AM,

[1] http://www.soda-pro.com/help/general-knowledge/linke-turbidity-factor

https://doi.org/10.26868/25222708.2021.30604

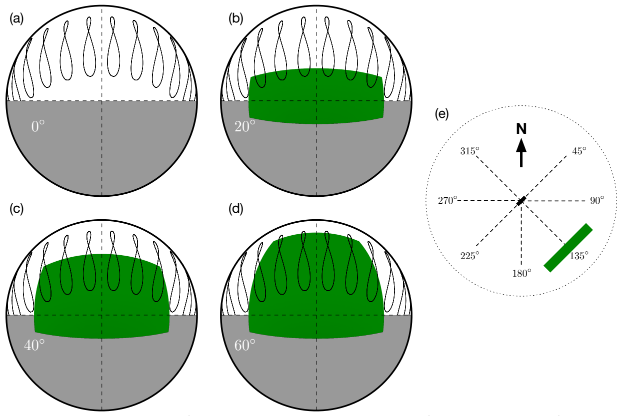

Figure 6: Insolation scenarios used to test relation between annual totals for SBI-airmass and direct sun irradiation: four degrees of obstruction (a) to (d), plus seven scene orientations (e)

respectively) were determined using a daylight coefficient matrix (DCM) for direct illumination which has 2056 light sources approximately evenly distributed across the hemisphere. At each time-step, the nearest DCM point to the actually occurring sun position (at that instant) is used for the calculation. For an annual simulation using the 2056 direct sun DCM, the displacement between actually occurring sun position and the nearest DCM point is typically $\sim 1.4°$ and never greater than $2.1°$. This spatial resolution (for the DCM) is commensurate with a temporal resolution in the time-step for the sun position of approximately 5.6 minutes. In other words, using time-steps as short as ~ 5 minutes are warranted on the basis of finely resolving the (continuous) path of the the sun using the 2056 direct sun DCM. Thus, time-steps shorter than 5 minutes would require a more finely grained DCM (say, 5000 points) to better resolve the sun position.

Results are shown for two weather files: Minneapolis (USA) and Paris (France) in Figure 7. Each plot of T_{wds} versus T_{sam} is annotated with a linear fit equation relating the two quantities, and a correlation coefficient for the fit. Of the seven orientations plotted (for each of the four obstruction cases), those for the surface orientations due east, south and west are highlighted with filled squares coloured red, green and blue, respectively. Immediately apparent in both plots is the strong correlation between T_{sam} and T_{wds}. Also evident is difference in slope between the two locations: sunnier Minneapolis has a slope of 0.549 whereas the slope for Paris is 0.257 (Figure 7). In both case the intercept is small enough to be considered equal to zero.

This simple relation between direct sun irradiation derived from weather files and airmass sunlight beam index means that measures of T_{sam} can be readily converted to absolute measures of direct sun irradiation (in kWh) using a *single* conversion factor derived from weather files. Note, in the ABDM schema, the

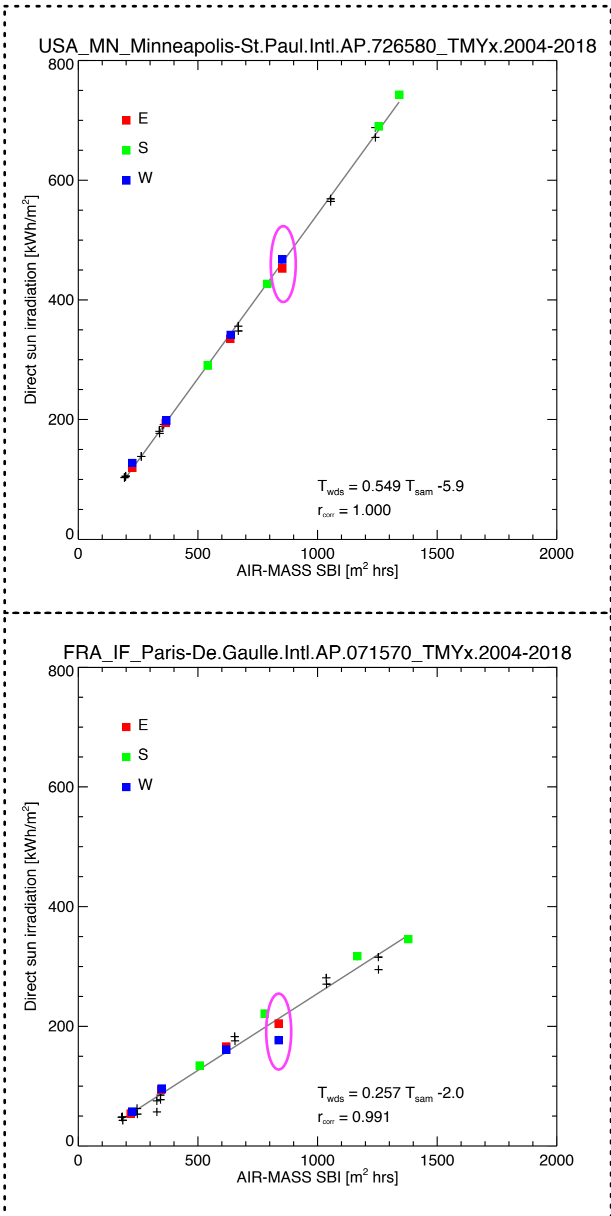

Figure 7: T_{wds} versus T_{sam} for Minneapolis (USA) and Paris (France) – 15 minute time-step

'aperture' is any planar surface on the building envelope – as well as a window opening, it could be an area intended for a PV panel (or indeed any solar dependant facade technology). For example, say an 8 m^2 surface intended for a PV array was predicted to have a T_{sam} of 9600 m^2 hrs for a location in Minneapolis, and 8800 m^2 hrs for Paris. The simple calculation to determine the direct solar irradiation yield would be as follows:

$$T_{wds} = 0.549 \times 9600 = 5270\,\mathrm{kWh} \quad \textbf{Minneapolis}$$

$$T_{wds} = 0.257 \times 8800 = 2262\,\mathrm{kWh} \quad \textbf{Paris}$$

This preliminary evaluation has, the authors believe, lent considerable support to the hypothesis that airmass SBI can serve as a reliable proxy for direct sun irradiation. A fuller evaluation is in preparation and

https://doi.org/10.26868/25222708.2021.30604

will be presented in the near future. The section that follows was not originally planned to be a part of this paper, and in many ways can be considered to be completely separate. However, these serendipitous observations were revealed in the course of deriving the (location specific) relation between T_{wds} and T_{sam}. Furthermore, given the potentially significant impact of the observations on the users of building simulation (practitioners and researchers), the authors felt it important to bring these findings to attention at the earliest possible opportunity.

Direct (ab)normal irradiation?

It was expected that there would be scatter in the plots of T_{wds} versus T_{sam} since the latter is essentially a continuous quantity which always has a non-zero value whenever any part of the 'aperture' can see any of the possibly occurring sun positions. Whilst the former, of course, contains many zero values and has a pattern which is subject to the vagaries of local conditions as derived from the original climate data which served as the basis for the weather files.

One observation in particular that stands out in some of the plots is the difference between T_{wds} values for east and west facing instances of the same obstruction case. When this occurs, the T_{wds} for the east facing surface will be vertically above (or below) the T_{wds} for the equivalent west facing surface – since the airmass SBI value T_{sam} will be the same for both. An instance of this is highlighted in both plots, though it markedly more evident for Paris than Minneapolis. This effect is observed to greater or lesser degrees in the other locations that were examined. A difference between south-east and south-west orientations also occurs to similar degrees.

Real differences between annual total east and west direct sun radiation must result from a prevailing difference in the diurnal profiles of direct normal irradiance. In other words, an overall tendency for a greater degree of occurrence and/or magnitude of direct sun in the morning compared to the afternoon, or vice versa. Observations have revealed such east-west asymmetries in direct sun irradiance, resulting from a variety of causes. For example, tropical sites may experience heavier cloudiness in the afternoon due to the daily accumulation of water vapour and aerosols in the atmosphere as the temperature increases during the day. Thus causing higher direct sun totals on the east compared to the west, e.g. Gueymard (1993). Conversely, some sites may be prone to regular occurrences in morning fog and/or and advection effects resulting in higher sun irradiances on a west facing surface compared to one facing east, e.g. Salazar et al. (2020). Around large cities, the diurnal patterns in locally generated pollution (e.g. from traffic) could also be a factor through the production of photochemical smog. All the proven instances of diurnal asymmetries at a handful of sites were revealed from exacting, high-frequency (e.g. 1 minute) measurements of direct solar irradiance. Such exacting measurements are <u>not</u> the basis of standardised weather files, see Brembilla et al. (2019). Instead, weather files are usually derived from much cruder observational data, e.g. cloud cover, with many of the parameters – including direct normal irradiation – generated by models rather than based on direct measurement.

A further observation regarding the diurnal effect in direct normal present in weather files is one which was *not* expected by the authors of this paper – namely, that the magnitude and even sense (i.e. east > west, or vice versa) of the effect could be dependent on the time-step used, e.g. hourly or interpolated sub-hourly. This was something of a surprise. The effect is illustrated in Figure 8 which shows two pairs of plots: the sun path (altitude vs. azimuth) and a temporal map of direct normal irradiance for the weather file at the source resolution of 1 hr (i.e. 60 mins) and interpolated to a 15 min time-step. The

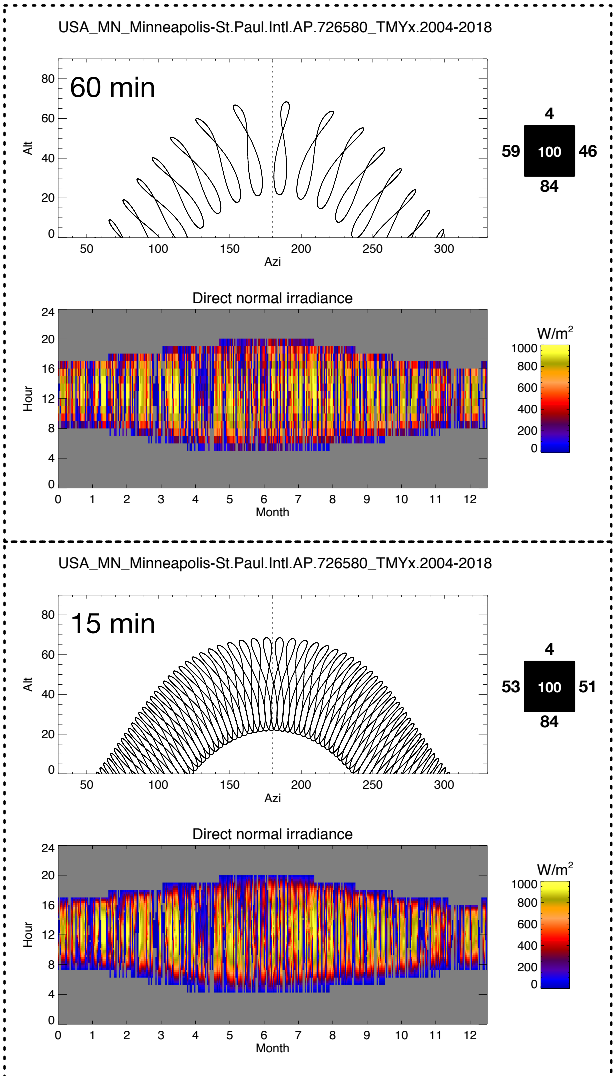

Figure 8: Minneapolis direct normal weather file at time-steps of 60 min (source) and interpolated to 15 min

https://doi.org/10.26868/25222708.2021.30604

box graphic to the right of sun path plot shows the annual total direct sun irradiation on the four (cardinal) vertical orientations normalised to that on the horizontal (= 100). This is calculated from first principles – through the absolute numbers are identical to the direct sun component predicted using the bespoke CBDM tool (as they should be for so straightforward a quantity). In going from the source resolution (i.e. hourly) to and interpolated time-step of 15 mins, the relative (and absolute) quantities on the north, south and horizontal surfaces do not change noticeably (i.e. >1%). However, the west:east ratio changes from 59:46 (60 min) to 53:51 (15 min) – from markedly different to barely noticeable.

The serendipitous discovery of this effect was investigated further to determine if it is often present in weather files, or simply due to the accidental choice of the first few investigated. Based on the twenty or so weather files from various sources, this east-west diurnal effect dependancy on (interpolated) time-step would appear to be commonplace. Thus far, the investigation has involved progressive halving of the time-step from the source value of 1 hr, to just under 1 min (i.e. 1, 1/2, 1/4, . . . , 1/64hr) and noting the effect on (annual total) east and west direct sun irradiation. Space restrictions preclude a full description of the initial findings, though the observations thus far can be summarised as follows. Most of the weather files tested showed a marked sensitivity to time-step with significant changes in the east west irradiation totals for direct sun – two are shown in Figure 9.

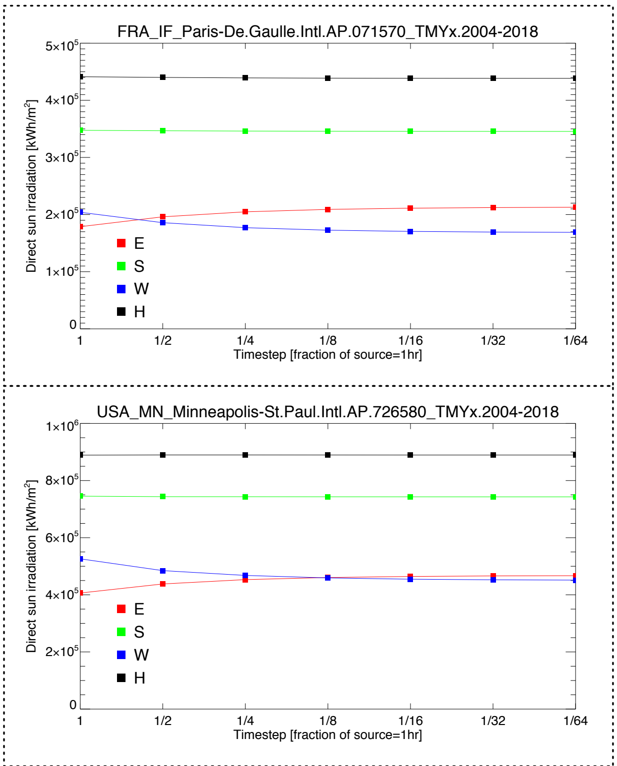

Figure 9: Direct normal versus time-step for Minneapolis and Paris

As is evident from the plots – time step has no noticeable effect on direct sun irradiation incident on the south and horizontal, but markedly so on the east and west. In both cases, the east and west irradiation totals appear to converge to stable values at time-steps around 1/16 hr or less (i.e. ∼4 min or shorter). This time-step effect on direct normal irradiation clearly requires some further investigation – the observed changes in east and west irradiation totals are in the region of about 20% or more of the totals for those orientations. Initial thoughts on the cause(s) for this effect are as follows. It appears to result from the effect of time-step on the sampling of the sun positions. This is illustrated in the altitude–azimuth plots for Minneapolis (Figure 8) where the pattern of the analemma at the source time-step (60 min) is clearly not symmetrical about the north–south axis, i.e. the dashed vertical line at azimuth 180°. The pattern for the analemma (with regard to symmetry about the north–south axis) will largely depend on the difference between local clock time and true solar time, with possibly some (small?) contribution depending on the equations used to calculate sun position. Superposed on that, of course, are the actual original values for direct normal irradiation in the (hourly) weather data.

The authors are not aware of any publications noting this effect of time-step on east-west direct irradiation, but it would be remarkable if hadn't been noticed previously. Inevitably, this observation brings into question the reliability of any prevailing differences in diurnal solar radiation present in standardised weather files. Put more bluntly: are these differences real, or are they the unintended consequence of the way the weather files are constructed? Should one assume that the converged values are correct? In which case, time-steps <10 min are required for those weather files that exhibit this effect. If so, a consequence of this would be an inherent unreliability in the solar radiation predictions on largely east and west facades which could have a significant bearing on simulation outcomes, e.g. overheating predictions, PV potential, etc.

Conclusion

This paper has described the airmass refinement for the sunlight beam index and shown that it can serve as a proxy for direct sun irradiation determined using weather files. For planning purposes, the validity and repeatability of the methodological basis for any daylight/sunlight evaluation are paramount. To have validity, the outcomes must relate meaningfully to the potential performance of actual spaces, e.g. both for the spaces in a proposed development, and the determination of the development's impact on the performance of existing spaces. Additionally, the method must not be subject to the vagaries of the 'performance gap' – otherwise it fails the repeata-

https://doi.org/10.26868/25222708.2021.30604

bility maxim, results will be contested, and decisions based on those results will be challenged in the courts. Also, an evaluation method for planning should be almost impossible to gameplay – accidentally or deliberately. The majority of existing planning guidelines and recommendations, including those in EN 17037 and (for the UK) the widely used BR 209 (Littlefair (2011)), cannot provide meaningful indicators for sunlight performance – in addition to crude methodology, the methods do not even take account of the sizes of windows.

The ABDM schema addresses these shortcomings by providing essentially purely geometrical measures of an aperture's potential to provide sunlight, skylight and views. The airmass refinement to the sunlight beam index provides the 'missing link' that allows airmass SBI values to be readily converted to irradiation totals derived from weather files. Thus, any 'performance gap' is highly constrained and (almost) eliminated entirely – the only requirement is that the direct normal irradiance (for any particular weather file) is a faithful representation of the *prevailing* sunlight conditions for that locale. This is largely assumed by many (most?) users of building simulation – practitioners and researchers. Nevertheless, the serendipitous observations reported in this paper indicate that the time-step effect should be investigated further. Note, the observed effect on east–west irradiation totals does not in any way undermine the SBI airmass refinement, nor its proposed application. Instead, it is an effect that needs to be understood, and possibly dealt with in any ongoing revision of weather files. Prevailing diurnal differences in solar radiation need to be: (a) founded on reliable observations; and, (b) represented robustly in the weather file time-series.

Research on the further development and application of ABDM will continue, in particular the calibration of (internal) performance measures (predicted using CBDM) against ABDM measures determined at the window aperture. The authors support the consideration of ABDM metrics as a replacement for the daylight/sunlight planning methods used in current guidelines such as EN 17037 and BR 209.

Acknowledgment

The authors gratefully acknowledge correspondence from Chris Gueymard (Solar Consulting Services) regarding causes of diurnal variations in direct solar radiation.

References

Brembilla, E., J. Mardaljevic, and A. Mylona (2019). Daylight simulation and compliance: Reliability of climate data solar radiation models. In *IBPSA - Building Simulation Conference*, Rome, Italy.

British Standards Institute (2018). BS EN 17037: 2018 – Daylight in buildings. *London, BSI.*

Enarun, D. and P. Littlefair (1995). Luminance models for overcast skies: Assessment using measured data. *Lighting Research and Technology 27*(1), 53–58.

Gueymard, C. (1993). Analysis of monthly average solar radiation and bright sunshine for different thresholds at Cape Canaveral, Florida. *Solar Energy 51*(2), 139 – 145.

Kasten, F. (1965). A new table and approximation formula for the relative optical air mass. *Archiv für Meteorologie, Geophysik und Bioklimatologie, Serie B 14*(2), 206–223.

Laue, E. (1970). The measurement of solar spectral irradiance at different terrestrial elevations. *Solar Energy 13*(1), 43 – 57.

Littlefair, P. (2011). *BR209 - Site Layout Planning For Daylight And Sunlight: A Guide To Good Practice 2nd Edition.* Building Research Establishment, Garston, UK.

Mardaljevic, J. (2017). Aperture Sunlight and Skylight Indices: A Rating System for Windows and Shading Devices. *CIBSE Technical Symposium, Loughborough, UK 5-6 April.*

Mardaljevic, J. (2020). Aperture-Based Daylight Modelling: A New Approach for Daylight and Sunlight Planning. *CIBSE Technical Symposium, Virtual 14-15 September.*

Mardaljevic, J. (Rome, Italy, 2019). Aperture-Based Daylight Modelling: Introducing the 'View Lumen'. *IBPSA - Building Simulation Conference*.

Mardaljevic, J. and N. Roy (2016). The sunlight beam index. *Lighting Research & Technology 48*(1), 55–69.

Mardaljevic, J. and N. Roy (2017). Envelope first / Inside later: Aperture Sunlight and Skylight Indices. *PLEA - Passive and Low Energy Architecture, Edinburgh, UK, 3 - 5 July*.

Meinel, A. B. and M. P. Meinel (1976). *Applied solar energy.* MA: Addison-Wesley.

Salazar, G., C. Gueymard, J. B. Galdino, O. de Castro Vilela, and N. Fraidenraich (2020). Solar irradiance time series derived from high-quality measurements, satellite-based models, and reanalyses at a near-equatorial site in Brazil. *Renewable and Sustainable Energy Reviews 117*, 109478.

https://doi.org/10.26868/25222708.2021.30604